

J.H. HONG\*, X.J. LIU\*, D.K. PARK\*, K.W. KIM\*, H.J. AHN\*, I.S. AHN\*<sup>‡</sup>

## SYNTHESIS AND ELECTROCHEMICAL CHARACTERISTICS OF MECHANICALLY ALLOYED ANODE MATERIALS SnS<sub>2</sub> FOR Li/SnS<sub>2</sub> CELLS

## SYNTEZA MECHANICZNA I CHARAKTERYSTYKA ELEKTROCHEMICZNA MATERIAŁÓW ANODOWYCH SnS<sub>2</sub> DLA OGNIW Li/SnS<sub>2</sub>

With the increasing demand for efficient and economic energy storage, tin disulfide (SnS<sub>2</sub>), as one of the most attractive anode candidates for the next generation high-energy rechargeable Li-ion battery, have been paid more and more attention because of its high theoretical energy density and cost effectiveness. In this study, a new, simple and effective process, mechanical alloying (MA), has been developed for preparing fine anode material tin disulfides, in which ammonium chloride (AC), referred to as process control agents (PCAs), were used to prevent excessive cold-welding and accelerate the synthesis rates to some extent. Meanwhile, in order to decrease the mean size of SnS<sub>2</sub> powder particles and improve the contact areas between the active materials, wet milling process was also conducted with normal hexane (NH) as a solvent PCA. The prepared powders were both characterized by X-ray diffraction, Field emission-scanning electron microscope and particle size analyzer. Finally, electrochemical measurements for Li/SnS<sub>2</sub> cells were taken at room temperature, using a two-electrode cell assembled in an argon-filled glove box and the electrolyte of 1M LiPF<sub>6</sub> in a mixture of ethylene carbonate (EC)/dimethyl carbonate (DMC)/ethylene methyl carbonate (EMC) (volume ratio of 1:1:1).

*Keywords:* MA, Li/SnS<sub>2</sub> cell, PCA, wet milling process and electrochemical characteristics

### 1. Introduction

Lithium secondary batteries, as power sources, have become an essential product in various energy device fields. In recent years, according to development of mobile devices such as cellular telecommunication tools, camcorder and notebook computer, extensive researches about anode active materials with high energy density have been performed to replace existing carbon anode [1-3]. Graphite as the most ubiquitous anode material used in lithium secondary batteries today, cannot meet the growing demand from high-energy application fields as a result of its low theoretical capacity (372mAhg<sup>-1</sup>) [4-6], thus, research and development on new alternative anode materials has become a top priority. Recently, tin (Sn) has been widely studied as an alternative material for the carbonaceous anode material in lithium secondary batteries since it has large theoretical capacity of 993mAh/g [7]. However, the reaction between tin and lithium causes great volume expansion of 358%. During the volume change, tin (Sn) particles are pulverized and electrically insulating film is formed on the surface of pulverized tin (Sn) particles. Then, the pulverized tin particle become dead volume that means electrical isolation [8]. In addition, studies on graphene nanosheets, single-layer graphite and a combination of graphene with semi-metals/metal oxides (ex. Sn, Si, SnO<sub>2</sub>), showing almost double the specific

capacity of graphite, have raised the prospect of the replacement of graphite anodes [9-14]. However, poor cycle stability caused by structural and morphological mismatches, has limited its application. It has been reported that transition metal sulfides, especially SnS<sub>2</sub> can be synthesized through direct combination of its constituent elements [15] or vapor transport [16,17] in sealed tubes at high temperatures (400-800°). However, these methods have been gradually disregarded due to the strict conditions required and the poor nanocrystalline structure of the final products [18]. Recently, the growth of SnS<sub>2</sub> nanostructures through hydrothermal and solvothermal methods has been widely accepted as it is very easy to control the composition, size and morphology of the resultant products [19-21]. Unfortunately, most of these techniques are relatively expensive and are not applicable for mass production [22-24]: either the adopted precursors and equipment are expensive, or they involve multi-step synthesis routes with optimal conditions that are difficult to provide, or the reactions are performed in the presence of solvents, in which a great deal of wastewater and by-products are formed, thus causing pollution of the environment and products, etc. In conclusion, it remains a big challenge to develop simple, reliable and economical synthetic routes for the synthesis of high-purity hierarchical SnS<sub>2</sub> powders.

\* SCHOOL OF NANO AND ADVANCED MATERIALS SCIENCE & ENGINEERING, AND LINC, GYEONGSANG NATIONAL UNIVERSITY, 900 GAJWA-DONG, JINJU, GYEONGNAM 660-701, KOREA

<sup>‡</sup> Corresponding author: ais@gnu.ac.kr

In this study, we prepared tin sulfide powder by mechanical alloying using tin powder and sulfur powder. Here, a process control agent (PCA), also referred to as a lubricant or surfactant, is added to the powder mixture during milling to reduce the effect of excessive cold-welding, as true alloying among powder particles can only occur when a balance is maintained between cold-welding and the fracturing of powder particles. Furthermore, the nature and amount of the PCA can greatly affect the powder particle size, grain size and even electrochemical activity, further affecting the cycle characteristics when used as anode materials.

## 2. Experimental procedure

### 2.1. Materials

Raw materials of tin powder (Sn, 99.9%, -325mesh) and sulfur powder (S, 99.9%, -100mesh) were purchased from Sigma-Aldrich Corporation, PCAs of ammonium chloride ( $\text{NH}_4\text{Cl}$ , >99.5%) and normal hexane ( $\text{CH}_3(\text{CH}_2)_4\text{CH}_3$ , 95.0%) were purchased from Samchun Pure Chemical Co., LTD. All chemicals except for hexane were dried in oven at  $60^\circ$  for 24h to remove water molecules adsorbed on the surface of the raw materials.

### 2.2. Synthesis of Anode Materials

According to the chemical formula for  $\text{SnS}_2$ , the raw materials (tin & sulfur) and grinding medium (stainless steel balls, 5 mm) were placed together into a jar in an argon-filled glove box. The atomic ratio of tin/sulfur is 1:2, the ball-to-powder ratio (BPR) is 20:1.

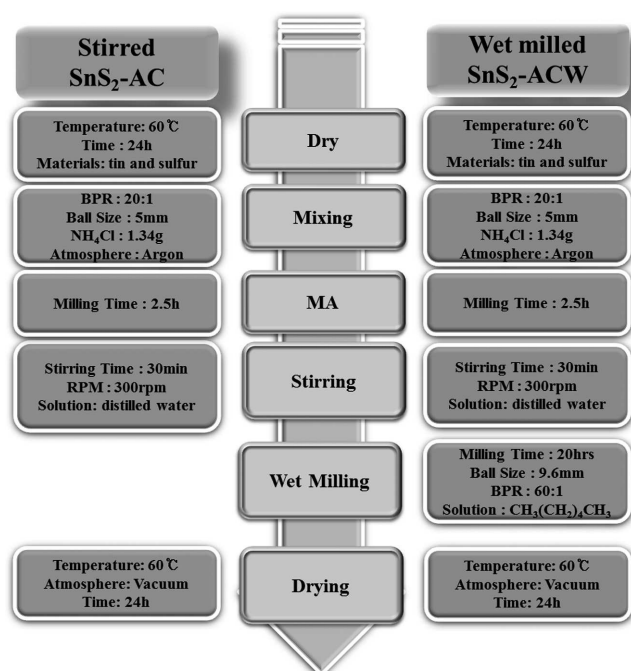


Fig. 1. Schematic of experimental procedure

Fig. 1 shows schematic of experimental procedure, in this study, two kinds of  $\text{SnS}_2$  have been prepared through almost the same drying, mixing, mechanical alloying process, used

process control agents (PCA-ammonium chloride ( $\text{NH}_4\text{Cl}$ )) and stirring was applied to wash off  $\text{NH}_4\text{Cl}$  with distilled water. And the only difference was added to wet milling process. Wet milling was conducted to decrease the mean particle size. After wet milling process and stirring, then dried at  $60^\circ$  under vacuum for 24hrs. In order to distinguish these two final products prepared for electrochemical testing, the former one using Ammonium Chloride (AC) is named  $\text{SnS}_2\text{-AC}$  and the latter one added wet milling process is named  $\text{SnS}_2\text{-ACW}$ .

### 2.3. Manufacture of Anode

The working electrodes were prepared by dispersing the active materials ( $\text{SnS}_2\text{-AC}$ ,  $\text{SnS}_2\text{-ACW}$ ), conductor (Super-P) and binder ((polyvinylidene fluoride) (PVDF)) into the organic solvent (N-Methylpyrrolidone (NMP)) with a mass ratio of 80:10:10. Then the homogeneous slurry was coated over the copper foil using a doctor-blade casting method, and dried in a vacuum oven for 24h. Furthermore, electrochemical measurements were taken using a two-electrode cell assembled in an argon-filled glove box, in which lithium was used as the counter and reference electrode, and a microporous polypropylene membrane of Celgard 2400 was used as a separator. The electrolyte was made by dissolving 1 M  $\text{LiPF}_6$  in a mixture of ethylene carbonate (EC)/dimethyl carbonate (DMC)/ethylene methyl carbonate (EMC) (volume ratio of 1:1:1).

### 2.4. Structure and morphology characterization

XRD measurements were carried out using a Philips PW3710 with  $\text{Cu K}\alpha$  radiation (RIGAKU, D/MAX-2500,  $\lambda = 1.5405\text{\AA}$ ). HELOS Particle Size Analysis was used to measure the size distribution, mean particle size and specific area of the alloyed powder, ranging from 250nm to  $87.5\mu\text{m}$ .

### 2.5. Electrochemical measurements

The charge/discharge measurements were taken on a WBCS 3000 Battery Tester between 0.01V and 2.5V, while cyclic voltammetry (CV) was conducted on a redefining electrochemical measurement at a scan rate of  $0.1\text{mVs}^{-1}$  between 0.01V and 2.5V vs.  $\text{Li}^+/\text{Li}$  at room temperature.

## 3. Results and discussion

Fig. 2 shows SEM micrographs of the starting materials of (a) sulfur, (b) tin, (c)  $\text{NH}_4\text{Cl}$ . Fig. 2 shows the original surface morphologies of the raw materials of tin and sulfur used in the experiment. The spherical shaped tin powders have a good size distribution, with the mean size of  $16\mu\text{m}$  shown in Fig. 2 (a), meanwhile the irregular shape of sulfur particles, which are relatively bigger were shown in Fig. 2 (b), and  $\text{NH}_4\text{Cl}$  with big particle size show in Fig. 2 (c). Fig. 3 is the SEM micrographs of synthesized  $\text{SnS}_2$  before and after wet milling, respectively. Clearly, the particle size was greatly decreased through wet milling process.

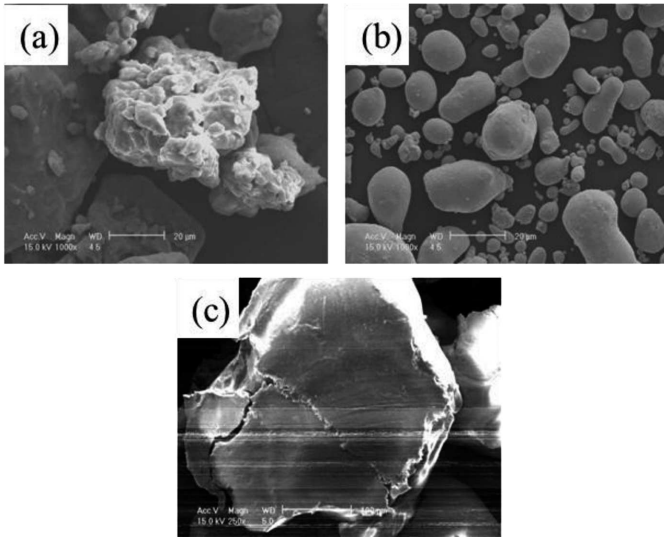


Fig. 2. SEM micrographs of the starting materials of (a) sulfur, (b) tin and (c)  $\text{NH}_4\text{Cl}$

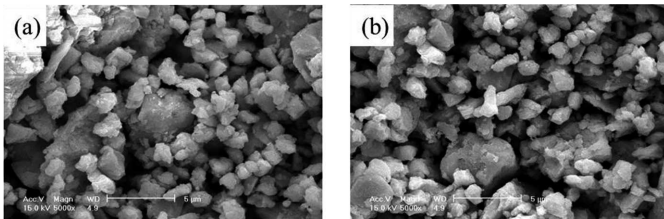


Fig. 3. SEM micrographs of synthesized  $\text{SnS}_2$  before and after wet milling

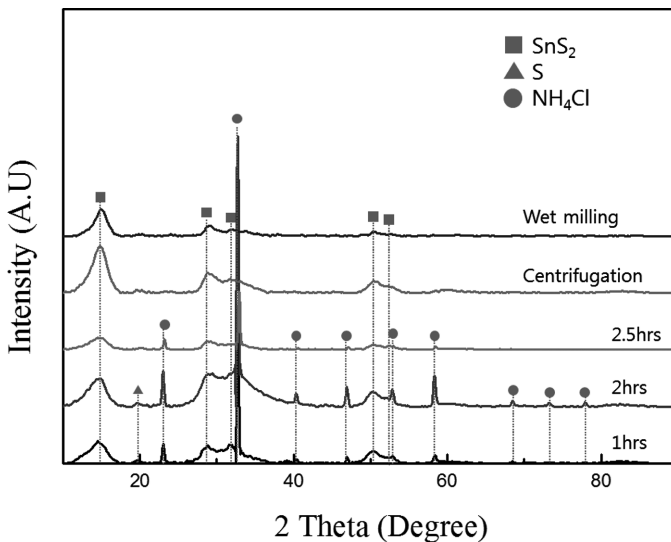


Fig. 4. XRD patterns of mechanical alloyed  $\text{SnS}_2$  powders with different milling times in the MA process and centrifugation and wet milling process

The crystal structures and phase transition of the as-prepared samples ( $\text{SnS}_2$ -AC, ACW) were confirmed by XRD. Fig. 4 shows XRD patterns of mechanical alloyed  $\text{SnS}_2$  powders with different milling times in the MA process, centrifugation and wet milling process. For  $\text{SnS}_2$ -AC, not only broad  $\text{SnS}_2$  peaks and small sulfur peaks were detected after 1h of milling, but also sharp  $\text{NH}_4\text{Cl}$  peaks, and the pattern

at 2.5h did not change much except for the disappearance of the small sulfur peaks, suggesting a complete reaction between the elemental reactants. The lack of any  $\text{NH}_4\text{Cl}$  peaks in the patterns of the stirred products confirmed that  $\text{NH}_4\text{Cl}$  was completely washed off through stirring. For  $\text{SnS}_2$ -ACW, the pattern is the same with the sample of  $\text{SnS}_2$ -AC, indicating that there were no impurities formed during the wet-milling process by comparing the wet-milled patterns with the same JCPDS card.

The cumulative distribution and density distribution curves for stirred  $\text{SnS}_2$ -AC, and wet-milled  $\text{SnS}_2$ -ACW powders are shown in Fig. 5 (a) and (b), respectively. Since the abscissa value of particle size corresponding to the ordinate value-50% of the cumulative distribution is defined as the mean particle size, according to the dotted line position, the average size of the above-mentioned powders are considered to be 7.66  $\mu\text{m}$  and 1.85  $\mu\text{m}$ . Obviously, wet-milling can not only disperse the agglomerated powder particles into small ones, but also improve their size distribution at the same time. The cumulative distribution curve of wet-milled  $\text{SnS}_2$ -ACW has always been on top of the dry milled one, suggesting the refinement of overall particles after wet ball milling. Referring to the density distribution curves, while stirred  $\text{SnS}_2$ -AC and wet-milled  $\text{SnS}_2$ -ACW have only one big peak respectively, indicating their good size distribution, which is conducive to the latter's electrochemical performance.

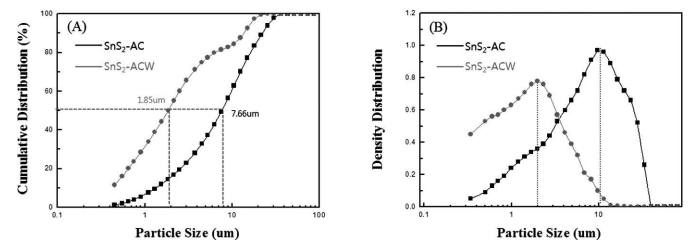


Fig. 5. Cumulative and density distribution curves of alloyed  $\text{SnS}_2$  powders before and after wet milling process

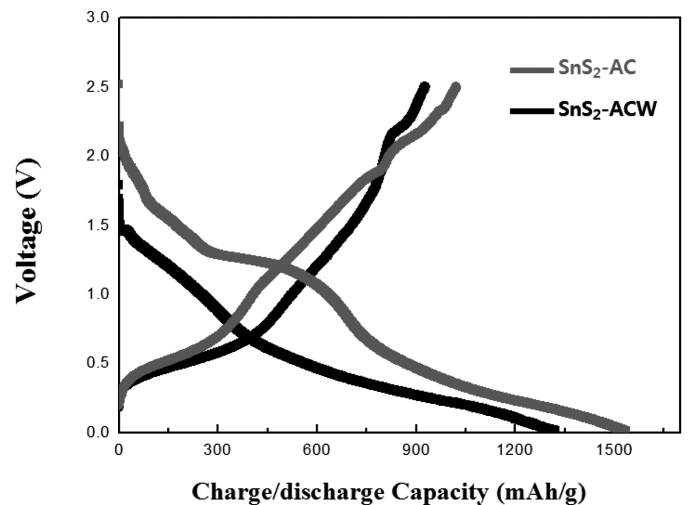


Fig. 6. The initial charge/discharge curves of Li/  $\text{SnS}_2$ -AC and Li/ $\text{SnS}_2$ -ACW cells

The initial charge/discharge curves of Li/ $\text{SnS}_2$ -AC and Li/ $\text{SnS}_2$ -ACW cells shown in Fig. 6 were measured with a current density of  $90\text{mA g}^{-1}$  between 0.01V and 2.5V, and

their corresponding charge/discharge capacities are 1021/1535 and 927/1322 mAhg<sup>-1</sup> ranged in a diminishing sequence from SnS<sub>2</sub>-AC to SnS<sub>2</sub>-ACW. And the irreversible capacities are attributed to the incomplete conversion reaction and irreversible loss of lithium ions due to the formation of Li<sub>2</sub>O and SEI.

The cycling performance were tested and shown in Fig. 7, clearly, the cell Li/SnS<sub>2</sub>-AC manifested extraordinary cycling behavior and retained a higher reversible capacity of 160 mAhg<sup>-1</sup> after 50 cycles, while for the cell of Li/SnS<sub>2</sub>-ACW, only 18mAhg<sup>-1</sup> was remained, mainly due to the long milling time. As known, the longer the milling conducted, the lower the crystallinity, therefore, the worse the cycling performance. In addition, another result that crystallinity played a much more important role than mean particle size on cycling performance can be obtained. Although the cycling performance is not so good when compared with other previous reports, AC, as an inorganic process control agent, was successfully applied into MA for the first time. Compared with the common organic SA, it not only can improve the crystallinity of synthesized tin sulfides, also shorten the milling time, thus providing a new way to prepare a series of metal sulfides in the future.

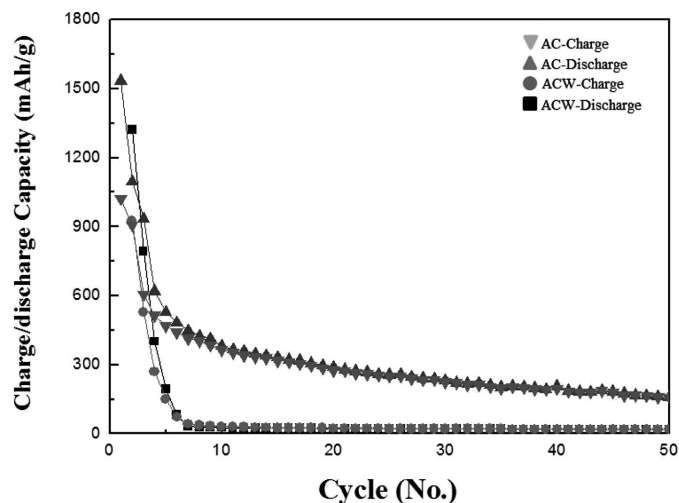


Fig. 7. The cycling performance of Li/ SnS<sub>2</sub>-AC and Li/SnS<sub>2</sub>-ACW cells at room temperature

#### 4. Conclusion

SnS<sub>2</sub> powder particles were synthesized through a new, simple and effective MA process, in which AC was used as a PCA to improve the alloying process at different levels and simultaneously affect the material properties. The structure, morphology and electrochemical performance of the as-synthesized powders were characterized by XRD, HELOS Particle Size Analyzer, and charge/discharge measurements. The stirred SnS<sub>2</sub>-AC, with better crystallinity but larger mean

particle size, presents a better reversible capacity and cycling performance than that of the wet-milled SnS<sub>2</sub>-SA, mainly due to its better crystal structural stability.

#### Acknowledgements

This research was supported by the National Research Foundation of Korea (NRF) grant funded by the Korea government (MEST) (No. 2012R1A2A2A02015831) and the Gyeongsang National University Fund for Professors on Sabbatical Leave, 2013.

#### REFERENCES

- [1] Y.Li, J.P. Tu, H.M. Wu, Y.F. Yuan, D.Q. Shi, *Mater. Sci. Eng. B* **128**, 75 (2006).
- [2] X. Liu, H.J. Ahn, I.S. Ahn, *J. Kor. Powd. Met. Inst.* **19**, 182 (2012).
- [3] J.W. Song, Otaduy Guillermo, S.J Hong, *J. Kor. Powd. Met. Inst.* **19**, 226 (2012).
- [4] M. Winter, R.J. Brodd, *Chem. Rev.* **104**, 4245 (2004).
- [5] Y.P. Wu, C. Jiang, C. Wu, R. Holze, *Solid State Ionics* **156**, 283 (2003).
- [6] W.J. Zhang, *J. Power Sources* **196**, 13 (2011).
- [7] Q.F. Dong, C.Z. Wu, M.G. Jin, Z.C. Huang, *Solid State Ionics*, **167**, 49 (2004).
- [8] Y.Li, J.P. Tu, X.H. Houang, H.M. Wu, Y.F. Yuan, *Electrochim. Acta* **52**, 1383 (2006).
- [9] A.K. Geim, K.S. Novoselov, *Nat. Mater.* **6**, 183 (2007).
- [10] E. Yoo, J. Kim, E. Hosono, H. Zhou, T. Kudo, I. Honma, *Nano Lett.* **8**, 2277 (2008).
- [11] B. Wang, X.L. Wu, C.Y. Shu, Y.G. Guo, C.R. Wang, *J. Mater. Chem.* **20**, 10661 (2010).
- [12] M. Pumera, *Chem. Rec.* **9**, 211 (2009).
- [13] G.X. Wang, X.P. Shen, J. Yao, J. Park, *Carbon* **47**, 2049 (2009).
- [14] Y.Q. Sun, Q.O. Wu, G.Q. Shi, *Energ. Environ. Sci.* **4**, 1113 (2011).
- [15] P.W. Shen, J.T. Wang, *Dictionary of Compounds*, Lexicographical Publishing House, Shanghai, 2002.
- [16] S.K. Arora, D.H. Patel, M.K. Agarwal, *Mater. Chem. Phys.* **45**, 63 (1996).
- [17] K. Kourtakis, J. DiCarlo, R. Kershaw, K. Dwight, A. Wold, *J. Solid State Chem.* **96**, 186 (1988).
- [18] H. Xiao, Y.C. Zhang, H.X. Bai, *Mater. Lett.* **63**, 809 (2009).
- [19] Y.C. Zhang, Z.N. Du, M. Zhang, *Mater. Lett.* **65**, 2891 (2011).
- [20] Y.C. Zhang, J. Li, M. Zhang, D.D. Dionysiou, *Environ. Sci. Technol.* **45**, 9324 (2011).
- [21] Y.C. Zhang, Z.N. Du, K.W. Li, M. Zhang, *Sep. Purif. Technol.* **81**, 101 (2011).
- [22] B. Hai, K. Tang, C. Wang, C. An, Q. Yang, Y. Qian, *J. Cryst. Growth* **225**, 92 (2001).
- [23] X.L. Gou, J. Chen, P.W. Shen, *Mater. Chem. Phys.* **93**, 557 (2005).
- [24] Q. Yang, K. Tang, C. Wang, D. Zhang, Y. Qian, *J. Solid State Chem.* **164**, 106 (2002).